Characteristics of Large Diameter, High-Density Helicon Plasma with Short Axial Length Using a Flat Spiral Antenna

Taisei MOTOMURA, Kenji TANAKA, Shunjiro SHINOHARA,
Takao TANIKAWA[1] and Konstantin P. SHAMRAI[2]

Interdisciplinary Graduate School of Engineering Sciences, Kyushu University, Kasuga, Fukuoka 816-8580, Japan
[1]*Research Institute of Science and Technology, Tokai University, Hiratsuka, Kanagawa 259-1292, Japan*
[2]*Institute for Nuclear Research, National Academy of Sciences, Kiev 03680, Ukraine*

A large diameter (up to 73.8 cm), high-density helicon plasma with short axial length (≤ 81 cm) has been successfully produced using a flat spiral antenna. The electron plasma density can reach up to $\sim 10^{13}$ cm^{-3} with the input radio frequency (rf) power of < 4 kW for various axial lengths, and the density scaling as a function of the axial length is in good agreement with expectations. The stronger the degree of magnetic field convergence from the antenna to the bulk plasma region is, the lower the minimum input rf power required to obtain a helicon plasma is. In the convergent magnetic field configuration, radial profiles of the excited rf magnetic field show the exicitation of higher order radial mode in addition to the component of the fundamental one. The manifestation of higher order mode is closely related to the magnetic field configuration and the rf radiation pattern of the flat spiral antenna.

Keywords: helicon plasma, density jump, high order radial mode, short axial length, flat spiral antenna

1. Introduction

High-density helicon plasmas [1-4] are potentially very useful in various plasma applications, such as in plasma processing, fusion, basic science fields including space plasmas and the development of magneto-plasma rockets. Using a helicon wave for plasma production gives advantages of having an easy operation and having a wide range of operational parameters. Developing a large volume plasma source with a large diameter is also important, and a high-density helicon plasma with very large plasma volume (up to 2.1 m³) has been obtained using a device at ISAS/JAXA (Institute of Space and Astronautical Science/Japan Aerospace eXploration Agency) [5-8].

However, having a shorter axial length with a large diameter (or a lower aspect ratio A, where A is the ratio of the axial length to the diameter) is often desirable in some of the above applications, e.g., the plasma processing and a magnetoplasma rocket. Therefore, using the same device at ISAS/JAXA, we have attempted to effectively shorten the plasma column length from 486 cm to as short as 12.5 cm by installing a termination plate inside the chamber [Fig. 1 (a)], reducing A from 6.6 to 0.17.

Here, we report the successful production of a high-density helicon plasma with $0.17 \leq A \leq 1.1$, which is much smaller than the aspect ratio of plasmas produced in conventional helicon sources. Note that although the axial length of the shortest helicon plasma ever produced is a mere 4.7 cm [9], the plasma

diameter is 2.5 cm, resulting in $A = 1.9$ that is larger than ours.
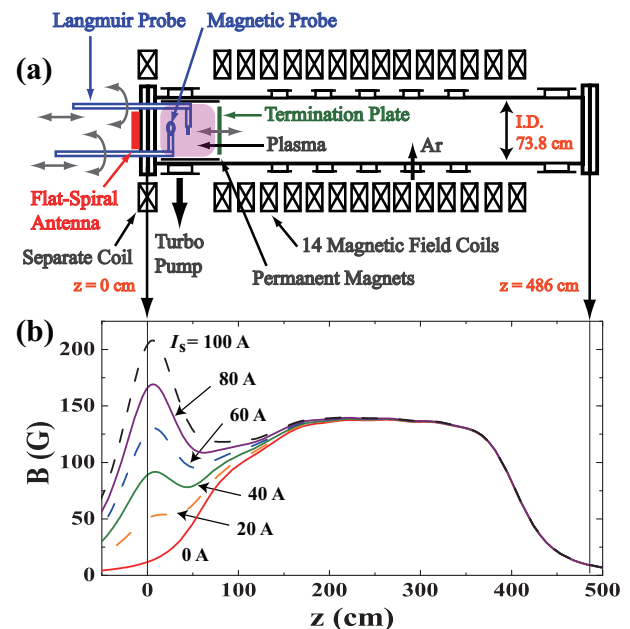
2. Experimental Setup

Fig. 1 (a) Schematic drawing of plasma device. (b) Axial magnetic field configurations for various values of the separate coil current I_s at radial position $r = 0$ cm.

In our device at ISAS/JAXA [5-8] [Fig. 1 (a)], the size of vacuum chamber is 73.8 cm in inner diameter and 486 cm in axial length. The magnetic field

is produced by 14 main coils and a newly installed separate coil which is located at the axial position of $z = 0$ cm. The magnetic field configuration near the antenna can be more flexibly controlled using this separate coil than using the old one used in the previous experiments [5-8], as shown in Fig.1 (b) (the 14 main coils generate the uniform axial field of 140 G in the central region). A 4-turn flat spiral antenna, 43 cm in diameter, is connected to the rf power supply (maximum power of 5 kW with 7 MHz excitation frequency) through a matching circuit. The rf radiation pattern from the antenna can be varied by changing the number of spiral turns used for plasma production as discussed in the previous papers [5-8]. The termination plate placed at $z_E = 12.5 - 81$ cm is made of a stainless steel punching plate, 0.5 mm thick, with a transparency of ~ 35 %, and is electrically floating (z_E is the axial position of the termination plate). Permanent magnets (the field strength at the surface is 1 kG) are installed at one end of the chamber to form a multi-mirror surface field inside the chamber [7]. A Langmuir probe and a magnetic probe are used to measure the spatial profiles of ion saturation current and the z-component of the excited rf magnetic field, respectively. The working gas is argon with a fill pressure of 0.75 mTorr.

3. Experimental Results

First, we show the case with full plasma axial length of 486 cm to estimate the effect of the short axial length. Figure 2 shows the electron density n_e as a function of the rf input power P_{in} for six different magnetic field configurations realized by changing the separate coil current I_s [see Fig. 1(b)]. The vertical bars show the threshold power P_{th}, at which the density jump from an inductively coupled plasma to a helicon plasma occurs. Typical values of n_e in helicon plasma discharge are $\sim 10^{13}$ cm^{-3} in all cases. With the increase in the magnetic field near the antenna, i.e., with the increase in I_s, the position of P_{th} becomes clearer and the value of P_{th} increases. Further increase in I_s (to 100 A) shows no density jump for $P_{in} \leq 4$ kW.

Figure 3 shows n_e as a function of P_{in} for two different axial lengths: $z_E =$ (a) 54.5 cm and (b) 34.5 cm. Similar to the 486 cm length case ([5-8] and Fig. 2), the position of P_{th} becomes clearer and the value of P_{th} increases even for the shorter axial length cases with the increase in I_s. These results are also consistent with the general tendency that the higher magnetic field (uniform field case) needs more rf power to have helicon jumps [10]. Note that the plasma production efficiency, N_e/P_{in} (N_e: total number of electrons) of $\sim 3 \times 10^{13}$ W^{-1}, is by more than one order of magnitude smaller than that of the 486 cm axial length
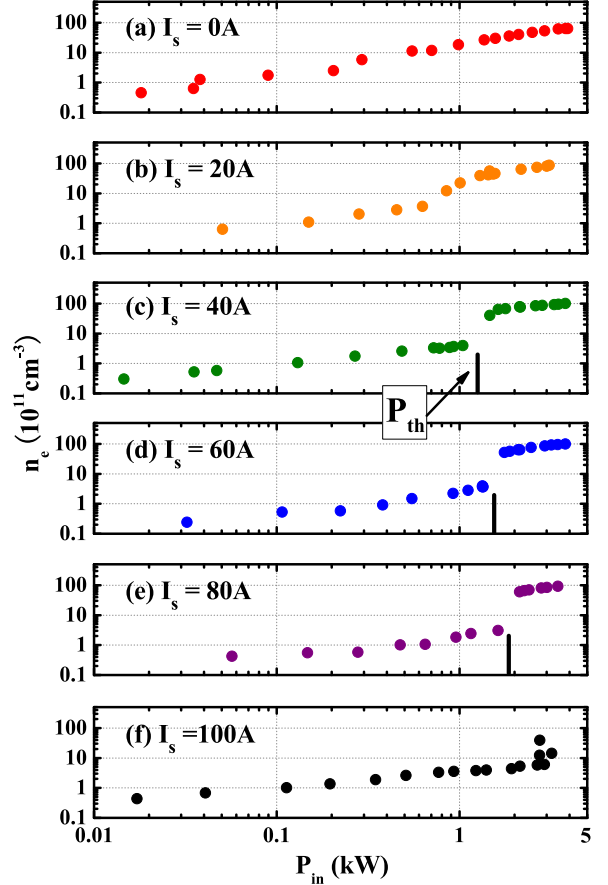

Fig. 2 Electron density n_e as a function of the rf input power P_{in} with 486 cm axial length for different values of the separate coil current I_s: (a) 0 A, (b) 20 A, (c) 40 A, (d) 60 A,(e) 80 A and (f) 100 A, respectively. A Langmuir probe is at radial position $r_p = 7.5$ cm and axial position $z_p = 31.5$ cm.

case: $\sim 10^{15}$ W^{-1}. This is due to the fact that shortening the axial length results in the enhancement of the axial ion loss relative to the radial one [8].

Figure 4 shows helicon plasma production efficiency N_e/P_{in} as a function of the axial plasma length L with $I_s = 20$ A and 60 A. For the case of a shorter axial length, the axial ion loss is much larger than the radial loss and is dominant. Therefore, N_e/P_{in} is expected to be proportional to L [8], which predicts the dotted line in Fig. 4 with a proportionality coefficient being roughly a factor of two lower than expected values [8]. From this, we can see a good agreement between the measurement and the prediction. We note that the values of N_e/P_{in} for our shorter axial length cases are still comparable or higher than those for the other small helicon devices (see Fig. 8 in [8]).

Figures 5(a) and 5(b) show the measurement of the radial and axial profiles of $\tilde{B}_z/|\tilde{I}_A|$, the ratio of excited rf magnetic field to rf antenna current amplitude, respectively. Profiles at twelve phases during
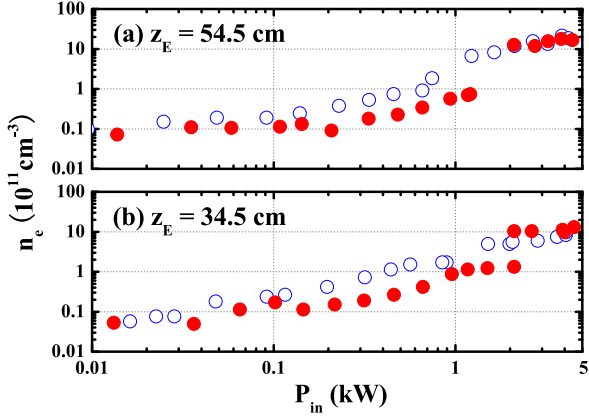
Fig. 3 Electron density n_e as a function of the rf input power P_{in} for different axial lengths: (a) $z_E = 54.5$ cm and (b) $z_E = 34.5$ cm. The open circles and black circles show the data taken at $I_s = 20$ A and $I_s = 60$ A, respectively. Here, the position of Langmuir probe is at $r_p = 0$ cm and (a) $z_p = 25$ cm and (b) $z_p = 15$ cm.
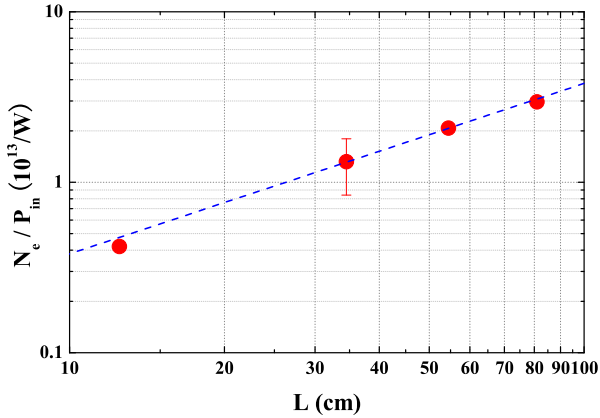

Fig. 4 Plasma production efficiency N_e/P_{in} (N_e: total number of electrons) in the helicon discharge as a function of the plasma length L. The dotted line is a predicted curve of $N_e/P_{in} \propto L$ to fit the experimental data. Typical error bar is also shown.
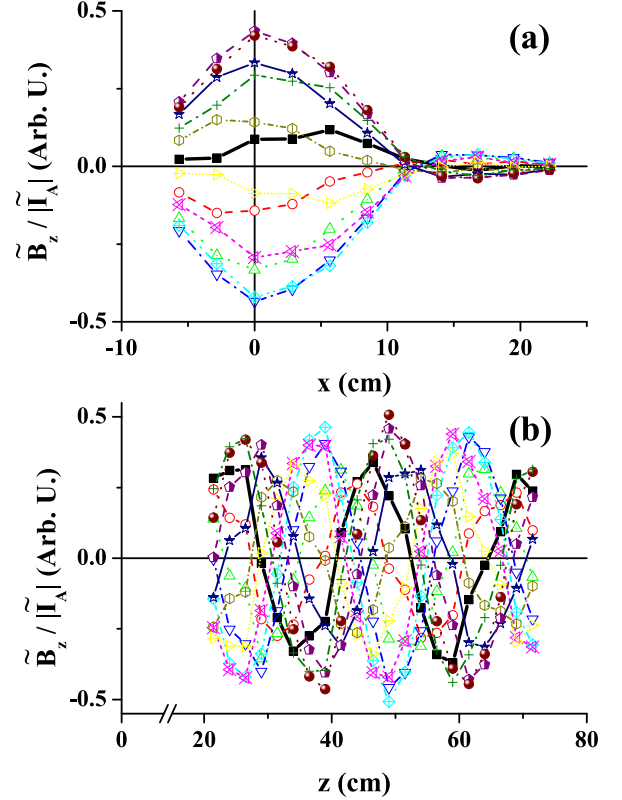

Fig. 5 (a) Radial and (b) axial profiles of the ratio of the excited rf magnetic field to the rf antenna current, $\tilde{B}_z/|\tilde{I}_A|$, with $I_s = 60$ A, $P_{in} \sim 1.9$ kW , $z_E = 81$ cm and the use of 2 turns (measurement). The magnetic probe is located at $z_p = 51.5$ cm for (a). Thick lines are used for an eye-guide.

one rf period at $I_s = 60$ A and $z_E = 81$ cm are shown. For comparison, Figs. 6(a) and 6(b) show the calculation of the radial and axial profiles of $\tilde{B}_z$, respectively, based on ref. [11] and the following discussions using the experimental values. Note that the vertical axis is normalized by the amplitude of the fundamental mode expressed as $J_0(k_{\perp 1}r)$, which will be described later.

Contrary to the expectations, the observed radial profile is not a simple fundamental mode of the Bessel function $J_0(k_{\perp 1}r)$ with m (azimuthal mode number) $= 0$, where, $k_{\perp j}a$ is the jth zero of the J_1 Bessel function (a: effective plasma radius). Our data can be expressed as a combination of at least two Bessel functions: $J_0(k_{\perp j}r)$ with $n = 1$ and 2 [12, 13]; the calcu-

lation results in Fig. 6(a) are in good agreement with the experimental ones in Fig. 5(a). In the calculation, the following parameters are used: the amplitude ratio of $J_0(k_{\perp 2}r)$ to $J_0(k_{\perp 1}r)$ terms is 0.51, and the phase difference at measurement position between the two waves of the fundamental and the 2nd order modes is -6.5 degree.

Generally, a pure standing wave is represented by the summation of propagating and reflected waves without the damping effect, meaning that their amplitudes are the same. Figure 6(b) shows the result of the calculation in which a damping propagating wave and partially reflected wave by the termination plate are summed up. In our calculation, the effects of the wave damping, the 2nd order radial mode, and the axial boundary (the termination plate with the reflection coefficient of 50 % is located at $z_E = 81$ cm) are included. It can be seen that the wave pattern as well as the parallel wave number obtained in the calculation [Fig. 6(b)] is nearly equal to that obtained in our experiment [Fig. 5 (b)].

Note that in the shortest case of $z_E = 12.5$ cm, the axial mode number of $\sim 3/4$ is excited, which can be understood from the free (fixed) boundary condition
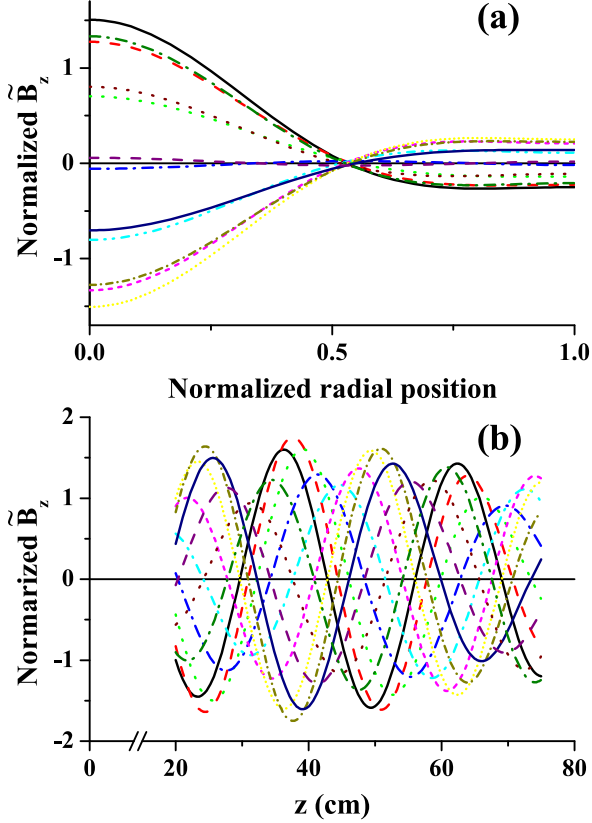
Fig. 6 (a) Radial and (b) axial profiles of $\tilde{B}_z$ (calculation). The amplitude ratio, (1st radial mode) / (2nd radial mode), is 1 / 0.51 and the phase difference between two modes at $z = 51.5$ cm is -6.5 degree. The wave reflection coefficient at the termination plate is 50% for the calculation of axial profile.

at the antenna side (termination plate) of $z = 0$ (12.5) cm, i.e., the axial mode number $n = 1/4 + p/2$ (p is the integer more than zero and here $p = 2$) can be excited from this boundary condition.

Figure 7 shows the axial profiles of $\tilde{B}_z/|\tilde{I}_A|$ for different magnetic field configurations (by changing I_s) and the different antenna radiation patterns. The contribution of the higher order radial modes becomes more important as I_s is reduced (i.e., the degree of the magnetic field convergence is stronger) and the number of antenna turns used is increased. It appears that the magnetic field configuration [14] and the radial density profile play very important roles in the excitation of the higher order radial modes. Preliminary theoretical results indicate that the excitation of the higher order radial modes is more significant with the peaked radial density profile. The next step is to fully understand the excitation mechanism of the higher order radial modes.

4. Conclusions

To summarize, we have successfully produced a large diameter (up to 73.8 cm), short axial length
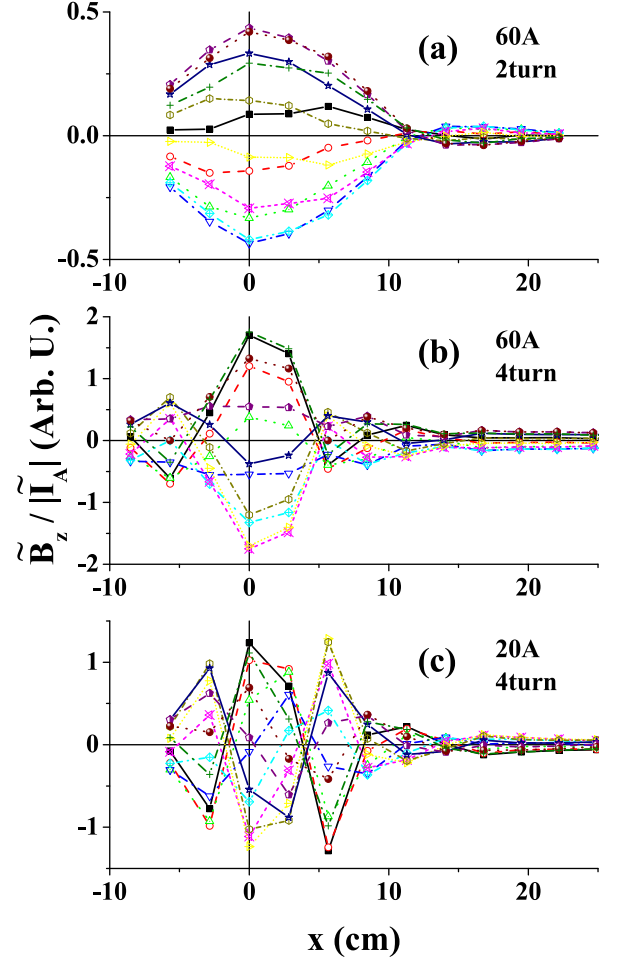

Fig. 7 Radial profiles of $\tilde{B}_z/|\tilde{I}_A|$ for two different magnetic field configurations by changing the separate coil current I_s and two antenna radiation patterns measured at $z_E = 81$ cm and $z_p = 51.5$ cm for three different cases. The separate coil current I_s, the number of antenna turns used, and the input rf power P_{in}, respectively, are: (a) 60 A, 2 turns and ~ 1.9 kW, (b) 60 A, 4 turns and ~ 3.4 kW, and (c) 20 A, 4 turns and ~ 1.7 kW.

(12.5-81 cm), high-density helicon plasma (up to $\sim 10^{13}$ cm^{-3}) with an rf power of < 4 kW, showing the $m = 0$ helicon wave structure. The magnetic field configuration near the antenna critically influences the plasma production. In the higher magnetic field strength near the antenna, the higher rf input power is necessary to achieve a helicon density jump. The plasma production efficiency N_e/P_{in} is $\sim 4 \times 10^{12} - 3 \times 10^{13}$ W^{-1}, which agrees with the expectations and is higher than that in the other small diameter machines. The excitation of higher order radial modes is considered to be related to the magnetic field configuration and the radial density profile.

5. Acknowledgements

[1] R.W. Boswell, Phys. Lett. **33A**, 457 (1970).

[2] S. Shinohara, Jpn. J. Appl. Phys. **36**, 4695 (1997).

[3] R. W. Boswell and F. F. Chen, IEEE Trans. Plasma Sci. **25**, 1229 (1997).

[4] F. F. Chen and R. W. Boswell, IEEE Trans. Plasma Sci. **25**, 1245 (1997).

[5] S. Shinohara and T. Tanikawa, Rev. Sci. Instrum. **75**, 1941 (2004).

[6] S. Shinohara and T. Tanikawa, Phys. Plasmas **12**, 044502 (2005).

[7] T. Tanikawa and S. Shinohara, Thin Solid. Films **506-507**, 559 (2006).

[8] T. Tanikawa and S. Shinohara, *Proceedings of the 12th International Congress on Plasma Physics* (Nice, France, 2004), http://hal.archives-ouvertes.fr/hal-00002013/en/.

[9] K. Toki, S. Shinohara, T. Tanikawa, I. Funaki and K. P. Shamrai,*the 28th International Conference Electric Propulsion* (Toulouse, France, 2003), IEPC 03-0168.

[10] S. Shinohara and K. Yonekura, Plasma Phys. Control. Fusion **42**, 41 (2000).

[11] F. F. Chen, Plasma Phys. Control. Fusion **33**, 339 (1991).

[12] M. Light, I. D. Sudit, F. F. Chen and D. Arnush, Phys. Plasmas **2**, 4094 (1995).

[13] Y. Sakawa, N. Koshikawa and T. Shoji, Plasma Sources Sci. Technol. **6**, 96 (1997).

[14] V. F. Virko, K. P. Shamrai, Yu. V. Virko and G. S. Kirichenko, Phys. Plasmas **11**, 3888 (1995).